JACS
JOURNAL OF THE AMERICAN CHEMICAL SOCIETY

Communication

pubs.acs.org/JACS

One-Pot Colloidal Chemistry Route to Homogeneous and Doped Colloidosomes

Xue-Wei Xu,[†] Xi-Mo Zhang,[†] Chao Liu,[†] Ying-Long Yang,[†] Jian-Wei Liu,[†] Huai-Ping Cong,[†] Chun-Hua Dong,[‡] Xi-Feng Ren,[‡] and Shu-Hong Yu*[,†]

[†]Division of Nanomaterials and Chemistry, Hefei National Laboratory for Physical Sciences at Microscale, Department of Chemistry, and [‡]Key Laboratory of Quantum Information, University of Science and Technology of China, Hefei, Anhui 230026, P.R. China

Supporting Information

ABSTRACT: Colloidosomes are usually produced from a series of building blocks with different sizes ranging from several nanometers to micrometers or various shapes, such as particles, microrods, and quantum dots. Colloidosomes can possess a variety of characteristics in terms of photics, electrology, mechanical strength, and selective permeability, derived from their building blocks. However, poor mechanical stability and complicated synthesis processes have limited the applications of colloidosomes. Here, we report a new one-pot colloidal chemistry route to synthesize phenol formaldehyde resin (PFR), Ag@PFR, and Au@PFR colloidosomes with high yields. The method can be modified to synthesize different kinds of doped colloidosomes with different components, which will provide a new approach to design colloidosomes with different functions.

Three-dimensional structures assembled from colloid spheres, including colloid clusters and crystals,[1] have attracted considerable interest. Colloidosomes are an important type of these superstructures, possessing a hollow structure and a shell composed of colloid particles closely connected with neighboring ones.[2] A series of colloidosomes could be achieved by using various materials as building blocks which have different sizes ranging from several nanometers to micrometers[3] and various shapes, such as microrods,[3e] particles,[3b,4] quantum dots,[3c,5] oligomeric patches,[6] and nanowires.[7] Accordingly, colloidosomes may retain important physical properties of their different components, such as fluorescence,[3c,5] electrical properties,[7] and magnetism.[3c,8] In a normal process, colloid spheres are synthesized in advance and then added to oil-in-water (or water-in-oil) emulsions to self-assemble at the interface. Finally, the solvent inside the colloidosomes is replaced by another solvent that is miscible with the solvent outside the colloidosomes.[1f] After further sintering, colloidosomes could be transferred to any fresh fluid.[3b,9] However, this synthesis process is quite complicated and difficult to operate. Therefore, simple and easy-to-operate methods need to be developed to increase the possibility of application of colloidosomes structures. To the best of our knowledge, a one-pot colloidal synthesis of this kind of unique homogeneous and doped colloidosomes has not been realized so far.

Herein, we report a one-pot colloidal chemistry route to synthesize elegant homogeneous and doped colloidosomes, which greatly simplifies the production processes reported previously and can be extended to directly synthesize other kinds of doped colloidosomes with different components by introducing presynthesized colloidal spheres to this reaction system.

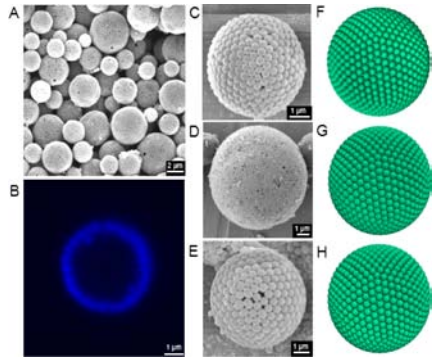

Figure 1. Structures of homogeneous and doped colloidosomes. (A) SEM image of PFR colloidosomes. (B) Confocal fluorescence microscopy image (excited by 400 nm) of PFR colloidosomes. (C−E) SEM images and (F−H) schematic illustrastions of homogeneous colloidosomes: (C,F) PFR colloidosomes, (D,G) Ag@PFR colloidosomes, and (E,H) Au@PFR colloidosomes.

This one-pot colloidal chemistry synthesis of colloidosomes was performed in a 50 mL Teflon-lined autoclave. A suitable amount of phenol monomer and hexamethylenetetramine (HMT) was dissolved in 45 mL of deionized water in the presence of polyethylene glycol (PEG, Mw = 20000). After being stirred mildly for ∼10 min, the solution was transferred into a Teflon-lined autoclave and hydrothermally heated at 160 °C for 4 h. A bright yellow colloidal solution was finally obtained. Typical scanning electron microscopy (SEM) images of obtained PFR colloidosomes are shown in Figure 1A,C. The PFR colloidosomes are assembled from PFR nanospheres[10] which have uniform sizes of ∼450 nm and are hexagonally close-packed (HCP) on the shell of colloidosomes. The PFR colloidosomes have a size distribution ranging from 1 to 6 μm (Figure 1A). A confocal fluorescence microscopy image (Figure 1B) confirms the hollow structure of PFR colloidosomes. A PFR colloidosome is illustrated schematically in Figure 1F.

Received: May 15, 2013
Published: August 9, 2013

dx.doi.org/10.1021/ja404880b | J. Am. Chem. Soc. 2013, 135, 12928−12931

The configuration of PFR nanospheres on shells of PFR colloidosomes is approximately HCP, although a few defects can be observed from the SEM images of colloidosomes. Meticulous research has been carried out on defects on the curved surface previously.[11] Packing defects are necessary for a six-fold-coordinated triangular lattice on a spherical surface owing to topological constraints on curved surfaces,[3b] and Euler's theorem shows that the total disclination charge of any sphere composed of triangular units must be 12. An ideal model—small spheres HCP on a curved surface to form a hollow structure—is built to study the relationship between the number (N) of small spheres composing colloidosomes and the radius ratio (r/R), where r and R refer to the radii of small spheres and colloidosomes, respectively. The number of small spheres assembling into colloidosomes can be calculated from the formula $N = 2\pi/(3A - \pi)$, with $A = \cos^{-1}\{[1 - 2(r/R)^2]/[2 - 2(r/R)^2]\}$, based on the ideal model. Comparing the ideal number with the actual number from manual counting, we find that the ideal model is consistent with the actual situation. The number of defects (defined as the difference between ideal and actual numbers of assembling spheres) increased largely with decreasing system size (r/R) (Supporting Information, Figure S1). There may be two reasons for that: on the one hand, the ideal model can be optimized further; on the other hand, some extra defects appear when the radius ratio decreases.

Unique Ag@PFR colloidosomes or Au@PFR colloidosomes were constructed from Ag@PFR or Au@PFR spheres, synthesized by adding $AgNO_3$ or $HAuCl_4$ into the initial reaction system, respectively (Figure 1D,E). Ag@PFR colloidosomes have a size distribution from 2 to 15 μm, while Ag@PFR spheres on Ag@PFR colloidosomes are ~300 nm in size. The average size of Ag@PFR nanospheres is less than the size of PFR spheres on PFR colloidosomes mainly because the amount of HMT for polymerization is less since some of HMT is used for reducing $AgNO_3$.[10] Au@PFR colloidosomes have structures similar to those of pure PFR colloidosomes (just using Au@PFR spheres in place of pure PFR spheres). Each Ag or Au nanoparticle encapsulated in the center of each sphere has a size of ~70 and 50 nm, respectively (Figure S2a,b).

Interestingly, when we add some pre-synthesized Ag@PFR spheres with a diameter of 900 nm into the initial reaction system, the Ag@PFR spheres join the newly formed PFR spheres, assembling into doped colloidosomes (Figure 2A). In the final doped colloidosomes, an Ag@PFR sphere sticks into the inner surface of the colloidosomes, surrounded by newly formed PFR spheres, similar to a cherry on a round cake. We define these novel superstructures as "doped Ag@PFR-PFR colloidosomes", the former part referring to the inserted sphere and the latter part to the building block units. The morphology of the assembled structures is closely responsive to the dosage of added Ag@PFR nanospheres. At low dosage (0.1 mg Ag@PFR), the average diameter of the obtained doped colloidosomes is 3.7 μm, and the building blocks of PFR nanospheres are 550 nm in size (Figure 3A). The inserted Ag@PFR spheres are 1.2 μm in size, bigger than the initial spheres because they grow further by polymerization during the following reaction process. On increasing the amount of Ag@PFR spheres to 0.25 mg, the final product would shrink mildly but still exist as a hollow colloidosome (Figure 3B). The average diameter of doped colloidosomes reduced to 3.0 μm, but the size of PFR nanospheres increased to 630 nm. With further increases in the amount of Ag@PFR spheres, the hollow colloidosome structures would shrink further into cluster structures (Figure 3C) until dimer structures composed of one

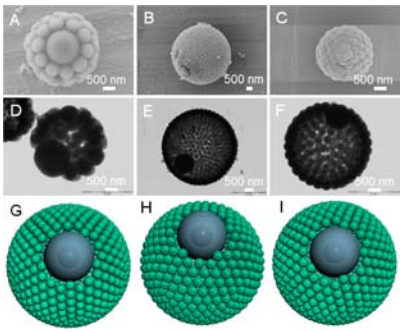

Figure 2. Structures of doped colloidosomes. The first, second, and third rows are SEM images, TEM images, and schematic illustrations of doped colloidosomes, respectively: (A,D,G) Ag@PFR-PFR doped colloidosomes; (B,E,H) Ag@PFR-Ag@PFR-doped colloidosomes; and (C,F,I), Ag@PFR-Au@PFR-doped colloidosomes.

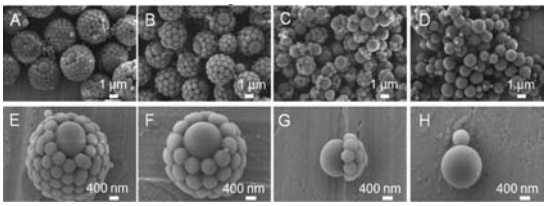

Figure 3. Shape evolution of the colloid clusters influenced by the amount of Ag@PFR spheres (diameter: 900 nm). The SEM images show final products with (top) low magnification and (bottom) high magnification: (A,E) 0.1 mg; (B,F) 0.25 mg; (C,G) 0.5 mg; and (D,H) 2.5 mg.

Ag@PFR sphere and one PFR sphere formed (Figure 3D). The size of the obtained PFR clusters and the number of assembled units were both reduced greatly compared with those of the former doped colloidosomes.

If we introduce $AgNO_3$ or $HAuCl_4$ to the initial solution while adding Ag@PFR spheres, it will generate a family of interesting doped colloidosomes such as Ag@PFR-Ag@PFR (Figure 2B) or Ag@PFR-Au@PFR (Figure 2C), respectively. Ag cores and Au cores in the correlative doped colloidosomes can be observed in Figure 2E, F, respectively. Ag@PFR-PFR, Ag@PFR-Ag@PFR and Ag@PFR-Au@PFR doped colloidosomes are illustrated schematically in Figure 2G, H and I, respectively. The size of the metal core can be adjusted easily from 50 to 100 nm by changing the amount of $AgNO_3$ (Figure S3). When we replace the pre-synthesized Ag@PFR spheres with other spheres, such as Au@PFR (Figure S4a,b) or polystyrene (PS) spheres (Figure S4c,d), doped colloidosomes with controllable components can also be synthesized. The reason for the change in the shape of PS spheres after the reaction needs further investigation.

The Fourier transform infrared (FTIR) spectra of PFR colloidosomes, PFR nanospheres, and PEG-20000 were measured at room temperature to study the interaction between PFR and PEG-20000. The band at 1230 cm^{-1}, which is attributed to C−O vibrations in PEG, confirmed that a PEG molecule remains in PFR colloidosomes (Figure S5a). The slight shift toward long wavelength may be due to bands between phenol formaldehyde resin and PEG. The solid-state ^{13}C NMR spectra of PFR colloidosomes, PFR nanospheres, and PEG-20000 also confirmed that some PEG molecules remianed in the final colloidosomes (Figure S5b). It is well known that PEG decomposes completely after being calcined in N_2 at 500 °C for 5 h, while PFR remains ~50 wt% weight of the initial product

dx.doi.org/10.1021/ja404880b | J. Am. Chem. Soc. 2013, 135, 12928−12931

at the same condition.[12] Comparing the residual obtained by calcination of PFR colloidosomes in O_2 with that calcined in N_2 (Figure S6), we can find that PEG molecule chains may be coated on surfaces of PFR nanospheres in the polymerization process. The size and number of PFR nanospheres on shells of colloidosomes can be adjusted by changing the amount of PEG (Figure S7). It can be inferred that PEG plays a crucial role in the whole formation process of the colloidosomes.

To investigate the formation mechanism of these elegant PFR colloidosomes and the crucial role of PEG in the synthesis process, we performed a series of control experiments. The freshly synthesized pure PFR spheres and homogeneous PFR colloidosomes were separated from the solutions, and their mother solutions were defined as solutions A and B, respectively. When we added PEG into solutions A and B and kept them continuously reacting at 160 °C for 4 h, PFR colloidosomes with similar assembled structures were obtained (Figure S8a,b). However, the PFR nanospheres on the surface of the colloidosomes were not as uniform as those on the colloidosomes synthesized by the normal one-pot process. The exterior PFR nanospheres are not homogeneous, probably because the molecular weight of phenol formaldehyde oligomer surviving in the mother solution is not so uniform. After being reacted further for 4 h, those molecules with different molecular weight transformed into nanospheres with different sizes. When the synthesis of pure PFR spheres was finished, we directly added PEG into the final colloid solution (defined as solution C) and then kept them reacting at 160 °C for 4 h. The final products were just cross-linked aggregated nanoparticles, different from colloidosomes. Yet, when we added HMT and PEG into solution C, similar colloidosomes were obtained (Figure S8c). The reason of these phenomena may be the chemical equilibrium shift during polymerization. When the final products were removed from the reaction system or reactant such as HMT was added into the resulting colloid solution, the chemical equilibrium shifted to the positive reaction. Then, unreacted or newly added HMT decomposed to NH_3, offering gas bladder templates for self-assembly of PFR nanoparticles. As a result, PFR colloidosomes formed after all. When only PEG was added into solution C, only cross-linked aggregated nanoparticles were obtained (Figure S8d). The reason may be that the chemical equilibrium did not shift and no NH_3 gas bladders formed in the subsequent reaction. Based on these facts, we believe that gas bladders formed by NH_3 are crucial and indispensable for the formation of colloidosomes. To get some direct evidence for the gas bladder mechanism, we reduced the amount of HMT. It was found that the structure of the obtained PFR colloidosomes was shrunk, just like shriveled basketballs (Figure S9). The reason may be that the internal pressure of the gas bubbles is too little to afford PFR spheres while the amount of HMT is reducing.

From the above results and observations, we propose a possible self-assembly mechanism in which *in situ* generated gas bladders provide an assembly interface for *in situ* formed colloidal PFR nanospheres, analogous to the process proposed previously: i.e., colloid particles were absorbed onto the gas/water or oil/water interface to reduce the system energy of foam or emulsion.[13] The whole formation process of PFR colloidosomes is illustrated in Scheme 1a. At first, HMT decomposed into HCHO and NH_3. HCHO polymerized with phenol, forming PFR spheres. As the polymerization process continued, the pressure inside the autoclave became higher because of continuously generated NH_3. When the pressure inside the autoclave was equal to the internal pressure of NH_3 gas bladders,

Scheme 1. Formation Mechanism of (a) Homogeneous and (b) Doped Colloidosomes

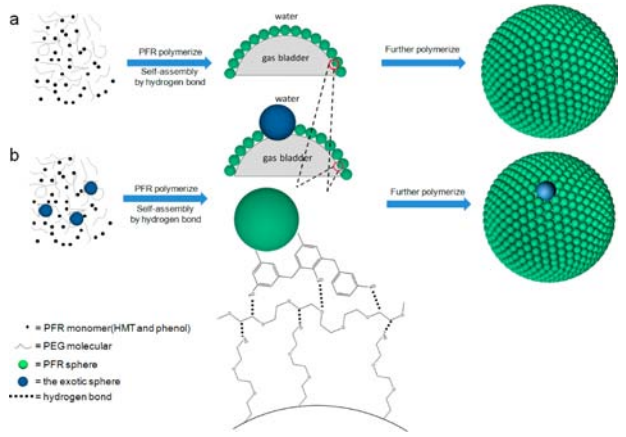

the gas bladders could remain unbroken and offer a stable gas/liquid interface for self-assembling PFR nanospheres. Synchronously, the phenol formaldehyde oligomer grew large enough to congregate into spheres. In this assembly process, PEG molecules not only could stabilize gas bladders by absorbing on their surfaces, but also could stick on the surface of PFR nanospheres and coat their surfaces with hydroxy groups. Next, PFR nanospheres are absorbed at the gas/water interface by hydrogen bonding, stabilizing the gas bladders. Such an assembly process is spontaneous because the total surface energy of the bladders reduces when colloid spheres adhere onto the interface. Owing to the presence of hydrophilic hydroxyl groups, most of PFR nanoparticles' bodies prefer to reside in water, which makes the particle monolayer curve to gas bladders and forms a gas-in-water emulsion.[13] As a result, the chain length of the PEG molecule is vital to the formation of PFR colloidosomes. If we change the molecular weight of PEG, colloidosome structures cannot be formed (Figure S10). When the reaction finished, the pressure in the autoclave reduced as the temperature of the reaction solution dropped. The gas bladder began to shrink, and PFR spheres on the gas/water interface pressed against the neighboring ones, forming stable colloidosomes.

The formation of Ag, Au@PFR colloidosomes is in direct contrast with the proposed formation mechanism. The structure of Ag, Au@PFR colloidosomes confirms that the self-assembly process occurs after Ag, Au@PFR spheres are formed. First, silver nanoparticles were formed by using HCHO as a reducing agent decomposed from HMT. Simultaneously, the polymerization reaction proceeded, and polymer layers were coated on silver particles, forming Ag@PFR nanoparticles. Those nanoparticles then assembled at the water/gas interface offered by the NH_3 gas bladders. As we know, the polymerization products of resorcinol and glucose also have a lot of hydroxy groups on their surface,[14] similar to the surface of PFR spheres polymerized from phenol. When we replaced phenol in the reaction system with resorcinol, the final products were dispersive PFR spheres with a few similar PFR colloidosomes (Figure S11a,b). The amount and structures of PFR colloidosomes with resorcinol may be improved in the future with accurate control. When we further replaced phenol with glucose, some carbon spheres with hollow structures appeared (Figure S11c,d). The hollow carbon spheres could be obtained from the gas templates generated from the decomposition of HMT.

dx.doi.org/10.1021/ja404880b | J. Am. Chem. Soc. 2013, 135, 12928−12931

As proposed above for the possible formation mechanism of colloidosomes, the assembly process took place just after the formation of PFR spheres. We propose that the formation mechanism of doped colloidosomes is similar to that of homogeneous colloidosomes (Scheme 1b). When PFR spheres formed in the reaction solution, the pre-synthesized Ag@PFR spheres could assembly at the gas/water interface together with newly formed PFR spheres. The equilibrium position of particles absorbed at the water/oil interface depends on the hydrophobicity of the particles surface.[15] Because the pre-synthesized Ag@PFR spheres were dried, the surface groups may be oxidated, and their surface may become hydrohobic. The equilibrium position of Ag@PFR spheres will tend to the gas phase. As a result, Ag@PFR spheres stick into the inner surface instead of protruding from the colloidosomes' outer surface. The position of Ag@PFR spheres will change with the diameter of PFR colloidosomes (Figure S12); the doped particle will protrude more outward with reducing diameter. The reason is that doped particles tend to maintain a constant contact angle on an interface. It is possible that the equilibrium position of large particles would move outward when the diameter of colloidosomes is decreasing.[16] When the amount of pre-synthesized Ag@PFR spheres increased, the amount of PFR spheres per Ag@PFR sphere decreased. As a result, the size of doped colloidosomes will be decreased with increasing amount of Ag@PFR spheres (Figure 3F). As the amount achieves a critical value, the gas bladder may not afford many heavy Ag@PFR spheres and may break out. In that case, PFR spheres may directly assembly on the surface of Ag@PFR spheres, forming a cluster structure (Figure 3G). When the amount of Ag@PFR spheres continues increasing, the final products may be Ag@PFR-PFR dimer structures (Figure 3H).

UV/vis spectroscopy was applied to study the optical properties of the PFR, Ag@PFR, and Au@PFR colloidosomes (Figure S13). The absorption peaks of Ag@PFR and Au@PFR colloidosomes between 600 and 800 nm are different from those of Ag@PFR and Au@PFR nanospheres, respectively. The reason for this may be the assembly of Ag@PFR and Au@PFR nanospheres on a curved interface.[17] The emission spectra show that PFR nanostructures have strong green fluorescence at 530 nm if excited by 340 nm (Figure S14). The introduction of surfactant PEG molecules can limit the degree of cross-linking of PFR in the synthesis process. Thus, PFR colloidosomes have lower fluorescence intensity compared with PFR spheres because the fluorescence will be reduced with decreased cross-linking of the polymer matrix.[18] In addition, the Ag and Au cores of colloidosomes will also inhibit the emission of PFR.

In summary, we have developed a one-pot colloidal chemistry route to synthesize unique homogeneous and doped colloidosomes. The formation mechanism of PFR colloidosomes could be a polymerization process simultaneously and synchronously coupled with a self-assembly process at a water/gas interface. This method can be extended to design elegant Ag or Au@PFR colloidosomes encapsulated with silver or gold nanoparticles in each nanosphere by introducing $AgNO_3$ or $HAuCl_4$. Furthermore, by adding pre-synthesized spheres (such as Ag@PFR, Au@PFR, or PS spheres) into the initial reaction system, we can also synthesize doped colloidosomes integrated with different components and functions. This colloidal chemistry route provides a new general strategy for producing a variety of unique homogeneous and doped colloidosomes with tunable components and functionalities.

■ ASSOCIATED CONTENT

Supporting Information

Experimental procedures, SEM and TEM images, and FTIR, NMR, emission, and UV/vis spectra. This material is available free of charge via the Internet at http://pubs.acs.org.

■ AUTHOR INFORMATION

Corresponding Author

shyu@ustc.edu.cn

Notes

The authors declare no competing financial interest.

■ ACKNOWLEDGMENTS

S.H.Y. acknowledges funding support from the National Basic Research Program of China (Grant 2010CB934700), the National Natural Science Foundation of China (Grants 91022032, 91227103, 21061160492), and the Chinese Academy of Sciences (Grant KJZD-EW-M01-1).

■ REFERENCES

(1) (a) Chen, Q.; Bae, S. C.; Granick, S. *Nature* **2011**, *469*, 381. (b) Chen, Q.; Whitmer, J. K.; Jiang, S.; Bae, S. C.; Luijten, E.; Granick, S. *Science* **2011**, *331*, 199. (c) Kim, J.-W.; Larsen, R. J.; Weitz, D. A. *Adv. Mater.* **2007**, *19*, 2005. (d) Kim, S.-H.; Kim, S.-H.; Yang, S.-M. *Adv. Mater.* **2009**, *21*, 3771. (e) Lauga, E.; Brenner, M. P. *Phys. Rev. Lett.* **2004**, *93*, 238301. (f) Velev, O. D.; Lenhoff, A. M.; Kaler, E. W. *Science* **2000**, *287*, 2240.

(2) Kim, J.-W.; Fernández-Nieves, A.; Dan, N.; Utada, A. S.; Marquez, M.; Weitz, D. A. *Nano Lett.* **2007**, *7*, 2876.

(3) (a) Bon, S. A. F.; Cauvin, S.; Colver, P. J. *Soft Matter* **2007**, *3*, 194. (b) Dinsmore, A. D.; Hsu, M. F.; Nikolaides, M. G.; Marquez, M.; Bausch, A. R.; Weitz, D. A. *Science* **2002**, *298*, 1006. (c) Duan, H.; Wang, D.; Sobal, N. S.; Giersig, M.; Kurth, D. G.; Möhwald, H. *Nano Lett.* **2005**, *5*, 949. (d) Lee, D.; Weitz, D. A. *Small* **2009**, *5*, 1932. (e) Noble, P. F.; Cayre, O. J.; Alargova, R. G.; Velev, O. D.; Paunov, V. N. *J. Am. Chem. Soc.* **2004**, *126*, 8092.

(4) (a) Lee, D.; Weitz, D. A. *Adv. Mater.* **2008**, *20*, 3498. (b) Wang, C.; Liu, H.; Gao, Q.; Liu, X.; Tong, Z. *ChemPhysChem* **2007**, *8*, 1157.

(5) Skaff, H.; Lin, Y.; Tangirala, R.; Breitenkamp, K.; Böker, A.; Russell, T. P.; Emrick, T. *Adv. Mater.* **2005**, *17*, 2082.

(6) Kim, D.; Kim, E.; Kim, J.; Park, K. M.; Baek, K.; Jung, M.; Ko, Y. H.; Sung, W.; Kim, H. S.; Suh, J. H.; Park, C. G.; Na, O. S.; Lee, D.-k.; Lee, K. E.; Han, S. S.; Kim, K. *Angew. Chem.* **2007**, *119*, 3541.

(7) Patra, D.; Malvankar, N.; Chin, E.; Tuominen, M.; Gu, Z.; Rotello, V. M. *Small* **2010**, *6*, 1402.

(8) Samanta, B.; Patra, D.; Subramani, C.; Ofir, Y.; Yesilbag, G.; Sanyal, A.; Rotello, V. M. *Small* **2009**, *5*, 685.

(9) (a) Thompson, K. L.; Armes, S. P. *Chem. Commun.* **2010**, *46*, 5274. (b) Thompson, K. L.; Armes, S. P.; York, D. W. *Langmuir* **2011**, *27*, 2357.

(10) Guo, S.-R.; Gong, J.-Y.; Jiang, P.; Wu, M.; Lu, Y.; Yu, S.-H. *Adv. Funct. Mater.* **2008**, *18*, 872.

(11) (a) Lipowsky, P.; Bowick, M. J.; Meinke, J. H.; Nelson, D. R.; Bausch, A. R. *Nat. Mater.* **2005**, *4*, 407. (b) Fernandez-Nieves, A.; Vitelli, V.; Utada, A. S.; Link, D. R.; Marquez, M.; Nelson, D. R.; Weitz, D. A. *Phys. Rev. Lett.* **2007**, *99*, 157801.

(12) Zhang, X.; Hu, H.; Zhu, Y.; Zhu, S. *J. Membr. Sci.* **2007**, *289*, 86.

(13) Mao, Z.; Xu, H.; Wang, D. *Adv. Funct. Mater.* **2010**, *20*, 1053.

(14) Sevilla, M.; Fuertes, A. B. *Chem.—Eur. J.* **2009**, *15*, 4195.

(15) Zeng, C.; Bissig, H.; Dinsmore, A. D. *Solid State Commun.* **2006**, *139*, 547.

(16) Zeng, C.; Brau, F.; Davidovitch, B.; Dinsmore, A. D. *Soft Matter* **2012**, *8*, 8582.

(17) Liu, J.-W.; Zhang, S.-Y.; Qi, H.; Wen, W.-C.; Yu, S.-H. *Small* **2012**, *8*, 2412.

(18) Song, J. C.; Neckers, D. C. *Polym. Eng. Sci.* **1996**, *36*, 394.